

Supporting Information

Boron doped carbon nanodots dispersed on graphitic carbon as high performance catalysts for acetylene hydrochlorination

Yuxue Yue,^{a†} Bolin Wang,^{a,b†} Saisai Wang,^a Chunxiao Jin,^a Jinyue Lu,^a Zheng Fang,^a Shujuan Shao,^a Zhiyan Pan,^b Jun Ni,^a Jia Zhao*^a and Xiaonian Li*^a

a. Industrial Catalysis Institute of Zhejiang University of Technology, State Key Laboratory Breeding Base of Green Chemistry-Synthesis Technology, Hangzhou, 310014, People's Republic of China.

b. Department of Environmental Engineering, Zhejiang University of Technology, Hangzhou, 310014, People's Republic of China.

*Corresponding author. Tel: +81 571 88871656. E-mail address: jiazhao@zjut.edu.cn; xnli@zjut.edu.cn.

Experimental

1.1 Materials

1-entyl-3-methylimidazolium tetrphenylborate (termed as [EMim][TPB]) and 1-entyl-3-methylimidazolium bis(trifluoromethylsulfonyl)imide (termed as [EMim][NTf₂]) ionic liquids were purchased from Lanzhou Greenchem, ILS, LICP, CAS (Lanzhou, China). Pristine Graphene (p-G) and boron oxide (B₂O₃) were purchased from Aladdin (Shanghai, China). Hydrogen chloride (HCl, 99.99%) and nitrogen (N₂, 99.9%) were used without further purification. The acetylene (C₂H₂) gas was purified by potassium dichromate solution to remove impurities, and then dried by zeolite-5A.

1.2 Preparation of B-CNDs materials

The B-CNDs materials derived from ionic liquids was prepared via a two-step method. Briefly, a homogeneous colloidal mixture was generated by performing a preassembly process with stirring and ultrasonic treatment for an ethanol solution containing 30 g [EMim][TPB] and 10 g [EMim][NTf₂]. The gelatinoids were then induced under nitrogen at 150 °C for 12 h to further promote the assembly between two ionic liquids and remove ethanol. Subsequently, the obtained mixture was calcined at 600 °C for 2 h under nitrogen at a heating rate of 10 °C. The carbonization process should be performed in a clean railboat. Finally, the materials of boron doped carbon nanodots (B-CNDs) was obtained. For comparison, the p-G material was treated with the same thermal treatment conditions (denoted as p-G-C).

The B-CNDs-g series materials was synthesized via a substitution reaction through carbonization of mixed pristine graphene and B₂O₃. Briefly, 2 g p-G and 1 g B₂O₃ were mixed under stirring in a deionized water for 10 min, followed by drying under nitrogen at 120 °C. Then the obtained mixture was transferred to a tubular furnace and calcined at 1000 °C for 2 h under N₂ at a heating rate of 10 °C min⁻¹. Subsequently, the obtained materials was washed by deionized water to remove the residual B₂O₃ and then dried under nitrogen at 120 °C. Finally, the obtained materials was termed as B-CNDs-g1. By the same method, catalysts calcined at 1200 and 1300 °C were prepared and named B-CNDs-g2 and B-CNDs-g3, respectively.

1.3 Catalysts test

For each catalytic test, 0.4 g of materials was loaded into a quartz tube fixed-bed reactor. The gas flow rate was controlled by mass flow controllers to maintain a total gas hourly space velocity (GHSV) of 1000 h⁻¹. All catalytic tests were evaluated using stoichiometric ratio of C₂H₂ to HCl of 1:1.2. The pressure for C₂H₂ and HCl is 0.06 MPa. The reaction gas stream was analyzed an on-line gas chromatograph (GC) equipped with a flame ionization detector (FID). A Porapak N packed column was used for permanent gas (C₂H₂ and VCM) separation followed with FID detector. The gas concentrations at each condition was measured with GC at least twice to make sure steady state was reached.

1.4 Characterization

The morphology and crystallinity of materials were characterized by transmission electron microscopy (TEM) equipped with a high-angle annular dark-field (HAADF) detector. The Raman spectra were examined on a Renishaw inVia Raman microscope. X-ray photoelectron spectroscopy (XPS) measurements were carried out using a Kratos AXIS Ultra DLD spectrometer. The atomic concentrations of elements are calculated based on the peak area integration including the sensitivity factor for different elements. BET surface area was calculated from the isotherm using the Brunauer-Emmett-Teller equation. Pore size distribution was calculated based

on nonlocal density functional theory method on the basis of the adsorption branch. XRD measurements were performed on a PANalytical-X'Pert PRO generator. FT-IR spectra were conducted on a Fourier transform infrared spectrophotometer Nicolet 6700 (Thermal Fisher Nicolet Corporation, Waltham, America).

1.5 Computational Details

DFT calculations were carried out in ADF (the Amsterdam Density Functional) software by employing the classical carbon-based cluster models.¹⁻³ In order to study the possible geometries of substrates adsorption on B-doped carbon surface, four B-doping models containing g-B, BC₃, BC₂O, and BCO₂ bonding patterns (Figure S7) were constructed based on the XPS characterization. For comparison, a pure carbon surface model was also devised. The geometries considered are fully optimized and the nature of stationary points characterized by the frequency calculations at B3LYP (d, p) level. A triple- ζ plus polarization (TZP) basis set is employed for all elements. The adsorption energy E_{ads} is defined as: $E_{\text{ads}} = E_{\text{complex}} - (E_{\text{substrates}} - E_{\text{surface}})$, where E_{complex} , $E_{\text{substrates}}$, and E_{surface} represent the single point energies of the adsorption complex, the isolated substrate, and the carbon surface, respectively. NPA population analysis was conducted to investigate the atomic charge distribution of the undoped and B doped surfaces. All calculations were done without any symmetry constraint. This procedure has been proved to be reliable and widely used to evaluate the absorption and emission properties of nanoparticles and quantum dots.⁴⁻⁶

Table S1. Contents of different B-containing species in B-CNDs calculated from XPS results.

Peak	Position (eV)	Peak area (%)	FWHM ^a (eV)	Contents (%)
-BC ₃	190.8	166	2.35	60.2
-BC ₂ O	192.0	60	1.49	21.7
-BCO ₂	192.8	50	0.99	18.1

^a FWHM = full width at half maximum.

Table S2. Crystalline Parameter of various samples.⁷

Samples	Lattice spacing (nm)
B	0.31
BC	0.28
BC ₃	0.26
C	0.25

Table S3. ICP results of various catalysts.

Catalysts	Element contents (ppm)			
	Fe	Cu	Al	Ca
p-G	/	/	/	11
B-CNDs	15	/	37	24

Table S4. Contents of different B-containing species calculated from XPS results.

Catalysts	Contents (%)		
	-BC ₃	-BC ₂ O	-BCO ₂
B-CNDs	60.2	21.7	18.1
B-CNDs-g1	53.5	33.8	12.7
B-CNDs-g2	36.7	42.5	20.8
B-CNDs-g3	30.2	44.6	25.2

Table S5. Detailed content of different elements of various catalysts obtained from the XPS analyses.

Catalysts	Element contents (%)			
	B	C	N	O
p-G	/	93.73	/	5.27
B-CNDs	5.27	85.62	0.77	8.34
B-CNDs-g1	6.24	90.19	/	3.57
B-CNDs-g2	6.77	88.62	/	4.61
B-CNDs-g3	6.62	88.82	/	4.56

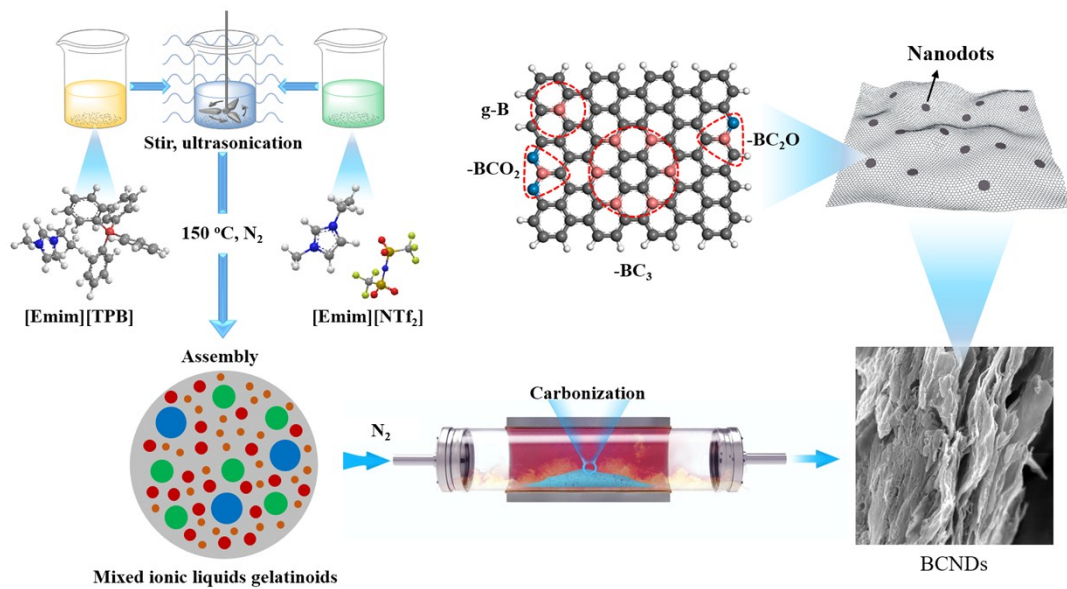
Table S6. STY of some selected outstanding metal-free catalysts for acetylene hydrochlorination.

Catalysts	Temperature; GHSV	STY ($kg_{VCM} kg_{Cat}^{-1} h^{-1}$) ^a	References
g-C ₃ N ₄ /AC	180 °C, 50 h ⁻¹	0.33	[8]
N-OMC-700	200 °C, 1 ml min ⁻¹	0.13	[9]
PSAC-N	250 °C, 120 h ⁻¹	0.11	[10]
SiC@N-C	200 °C, 0.8 ml min ⁻¹ g _{Cat} ⁻¹	0.09	[11]
B,N-G	250 °C, 36 h ⁻¹	0.29	[12]
PANI-AC	180 °C, 36 h ⁻¹	0.20	[13]
N-OMC-Ox	180 °C, 50 h ⁻¹	0.09	[14]
Z ₄ M ₁	180 °C, 50 h ⁻¹	0.15	[15]
AC-n-U500	210 °C, 50 h ⁻¹	0.18	[16]
p-BN	280 °C, 1.2 ml min ⁻¹	0.19	[17]
C-NH ₃	220 °C, 30 h ⁻¹	0.22	[18]
N-CNTs	180 °C, 180 h ⁻¹	0.02	[19]
N-MC-G	220 °C, 30 h ⁻¹	0.20	[20]
S, N-Carbon	180 °C, 50 h ⁻¹	0.19	[21]
ND@G	220 °C, 30 h ⁻¹	0.12	[22]
NC1-1073	180 °C, 120 h ⁻¹	1.63	[23]
C1100	220 °C, 36 h ⁻¹	0.38	[24]
NPC-800	180 °C, 1.7 ml min ⁻¹ g _{Cat} ⁻¹	0.26	[25]
MF-600	220 °C, 30 h ⁻¹	0.16	[26]
D-AC-M	220 °C, 2 ml min ⁻¹	0.15	[27]
3NR/4CAC	220 °C, 30 h ⁻¹	0.16	[28]
NP-C600	210 °C, 30 h ⁻¹	1.15	[29]
NS-C-NH ₃	220 °C, 2.6 ml min ⁻¹ g _{Cat} ⁻¹	0.40	[30]
B-CNDs	220 °C, 1000 h ⁻¹	1.19	This work

^a The STY calculated in this work was defined as follows:

$$STY = \frac{F_{C_2H_2} * 60 * Conv.\% * Sel.\% * M_{VCM}}{22400 * W_{Catal.}}$$

Where $F_{C_2H_2}$ stands for the gas flow of C₂H₂ (ml min⁻¹); *Conv.%* stands for the conversion of acetylene; *Sel.%* stands for the selectivity to VCM; $W_{Catal.}$ stands for the loading of catalysts (g); M_{VCM} stands for the molecular weight of C₂H₂ (g mol⁻¹); 22400 stands for the volume of 1mol gas in standard state (ml).



Scheme S1 The synthesis process of B-CNDs.

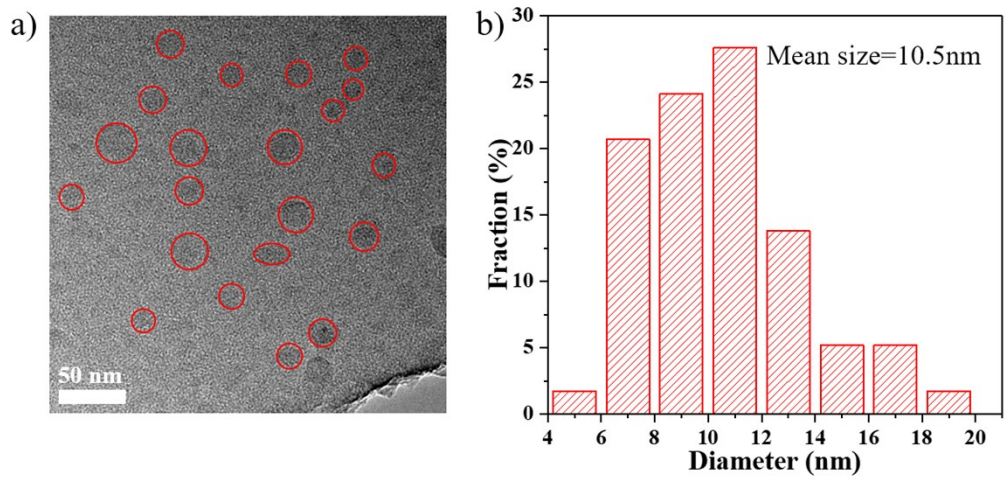


Figure S1 a) HRTEM image of B-CNDs. b) Size distribution of B-CNDs measured from a).

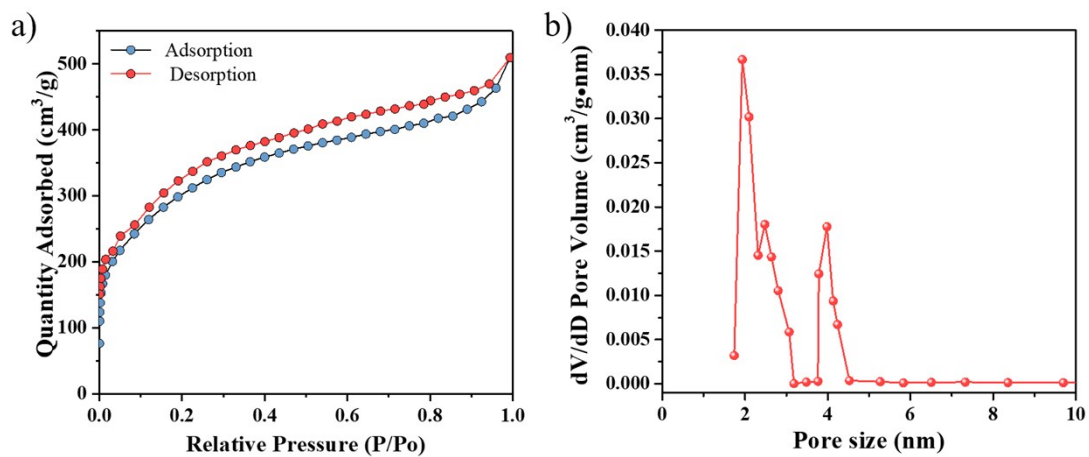


Figure S2 BET results of B-CNDs materials a) Nitrogen sorption isotherms and b) pore size distributions.

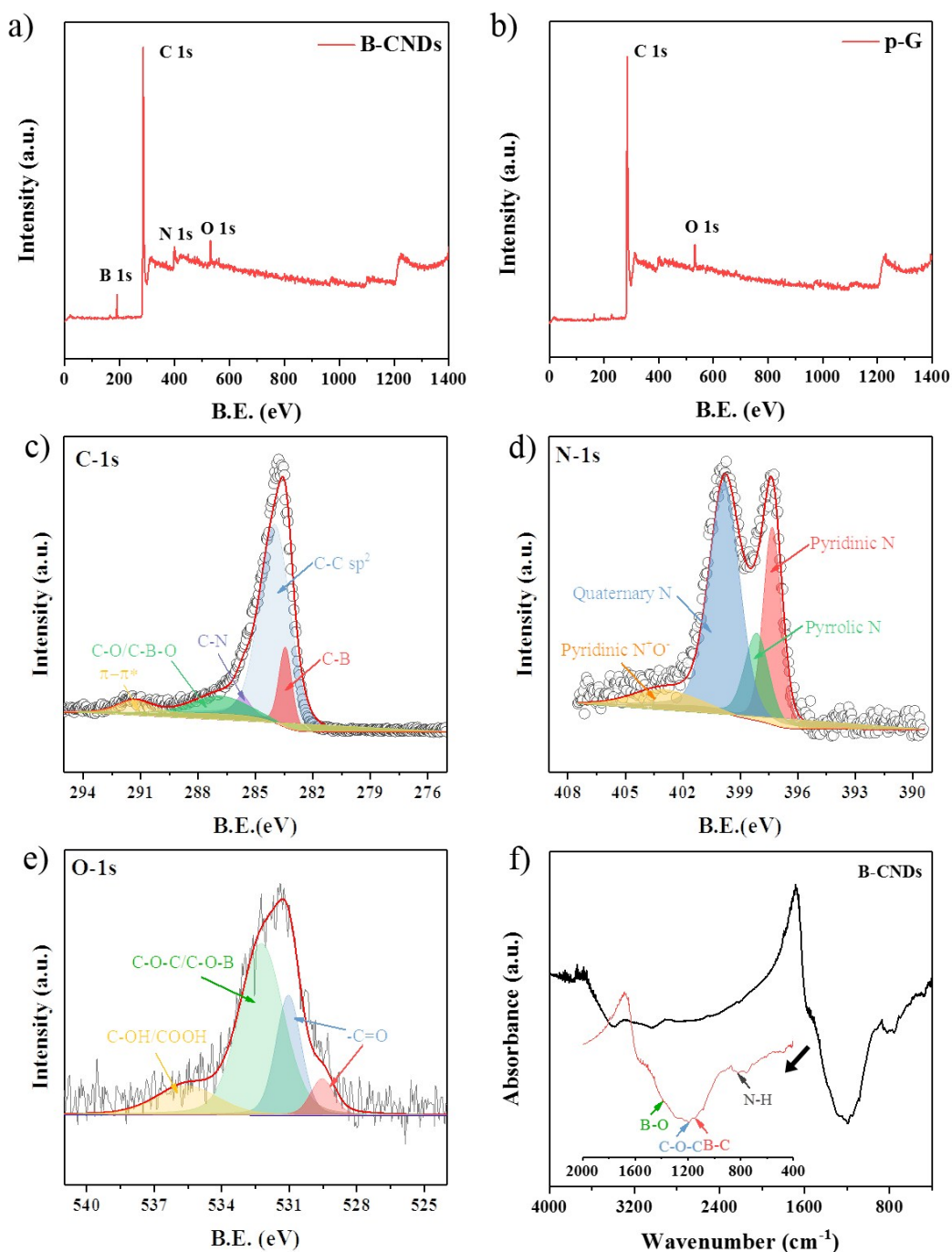
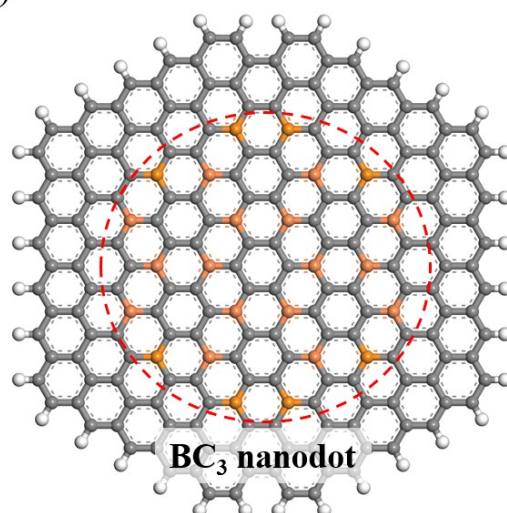


Figure S3 XPS survey scan of a) B-CNDs and b) p-G samples. XPS spectra of c) C-1s, d) B-1s and e) O-1s. f) FT-IR spectra of B-CNDs and (inset) FT-IR spectra of B-CNDs in the wavenumber range of 2000-400 cm^{-1} .

The C-1s XPS spectrum (Figure S3c) can be deconvoluted into C-B (BE = 283.4 eV), C-C (BE = 284.2 eV), C-N (BE = 285.5 eV), C-O (including C-O and C-B-O, BE = 286.4 eV) and π - π^* bonds (BE = 291.3 eV). The XPS N-1s spectrum of B-CNDs (Figure S3d) can be deconvoluted into four peaks. The peaks at 397.3, 398.2, 399.8 and 403.05 eV are attributed to the pyridinic nitrogen, pyrrolic nitrogen, quaternary N and pyridinic N⁺O⁻, respectively, without any N-B configuration (BE (binding energy) = 397.9 eV). As a result, a structure involving B-C species is very likely to exist in

B-CNDs. This is because the presence of its major components, C-B and C-C bonds, has already been justified from the XPS spectra, while N-B bonds cannot be observed in the N1s spectrum.

a)



b)

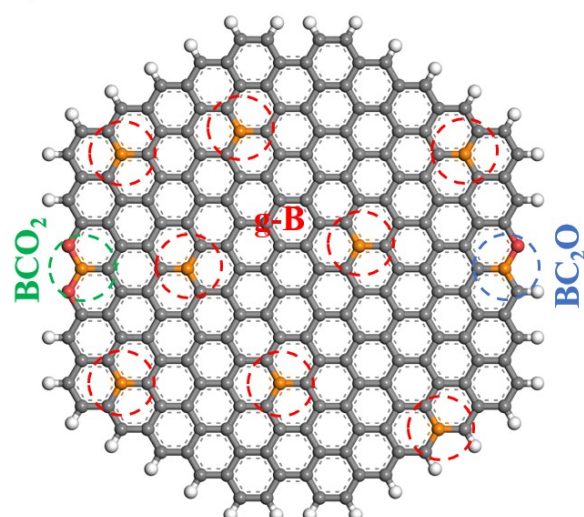


Figure S4 Schematic diagram of B species. The BC₃ in our manuscript indicates the structure that composed of a lot of boron and carbon atoms with an order arrangement like BC₃ nanosheets. The g-B structure indicates the disordered doping of boron atoms in graphene sheet. The dark, white, yellow and red balls indicate the carbon, hydrogen, boron and oxygen atoms, respectively.

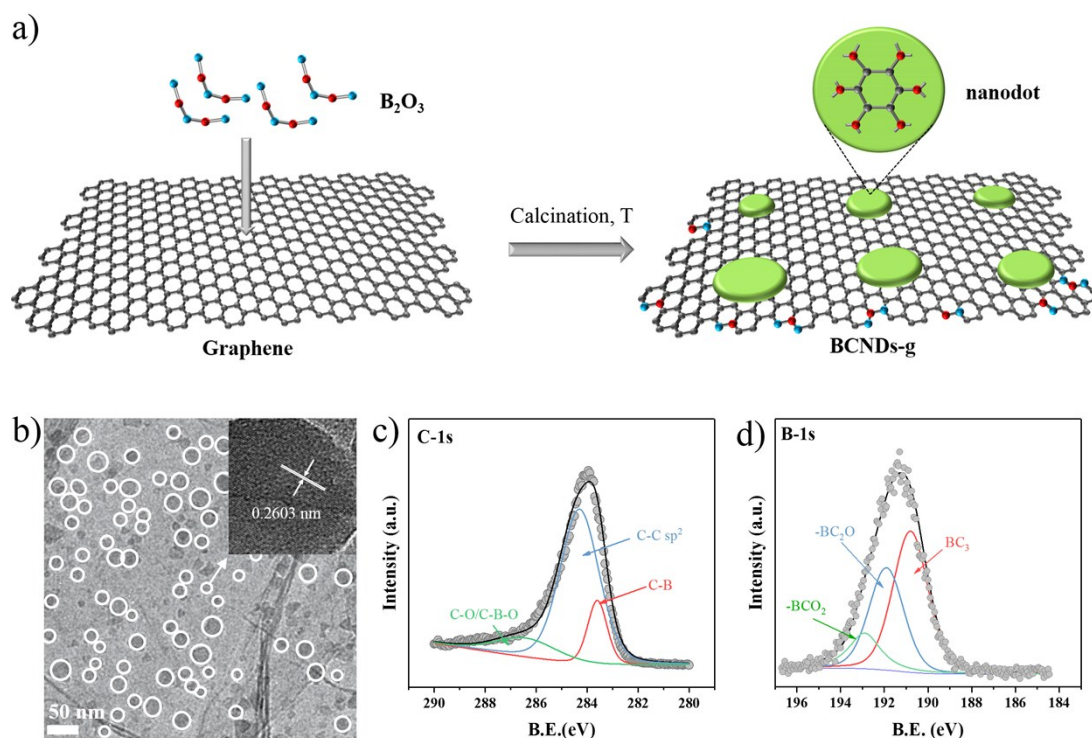


Figure S5 a) Synthesis of B-CNDs-g series catalysts via calcination of mixed graphene and B_2O_3 . Characterization results of B-CNDs-g1. b) HRTEM. c) C-1s and d) B-1s XPS spectra.

HRTEM image revealed the nanodots with crystal lattice embedded in graphene layer (Figure S5b), meanwhile, the observed lattice spacing is identical to the theoretical (200) lattice spacing of a BC_3 sheet, 0.2603 nm. XPS analysis was used to further investigate the chemical state of the nanodots on the surface of materials. The high resolution C-1s spectra for B-CNDs-g1 were fitted with three peaks at about 283.4, 284.2, and 286.4 eV, corresponding to C-B, C-C, and C-O/C-B-O, respectively (Figure S5c). The high resolution B-1s spectra for B-CNDs-g1 were fitted with three peaks at 190.8, 192 and 192.8 eV, corresponding to $-BC_3$, $-BC_2O$, and $-BCO_2$, respectively (Figure S5d). Their relative contents were 53.5 %, 33.8 %, and 12.7 %, respectively (Table S4). The above results confirmed the formation of $-BC_3$ nanodots in layered carbon materials for B-CNDs-g1, which is consistent with the B-CNDs materials that derived from ionic liquids.

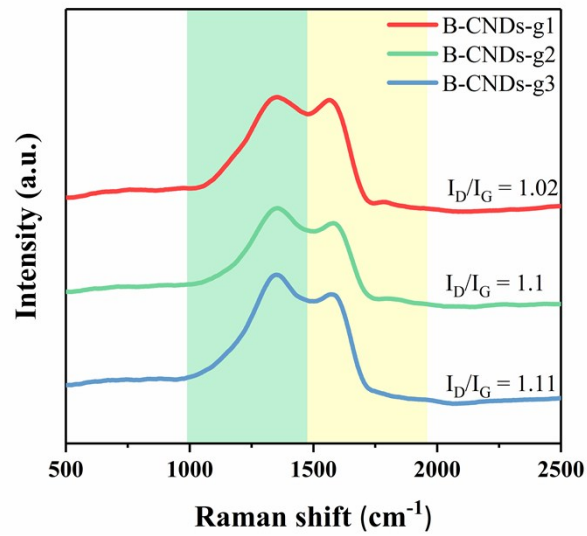


Figure S6 Raman spectrum of B-CNDs-g series materials.

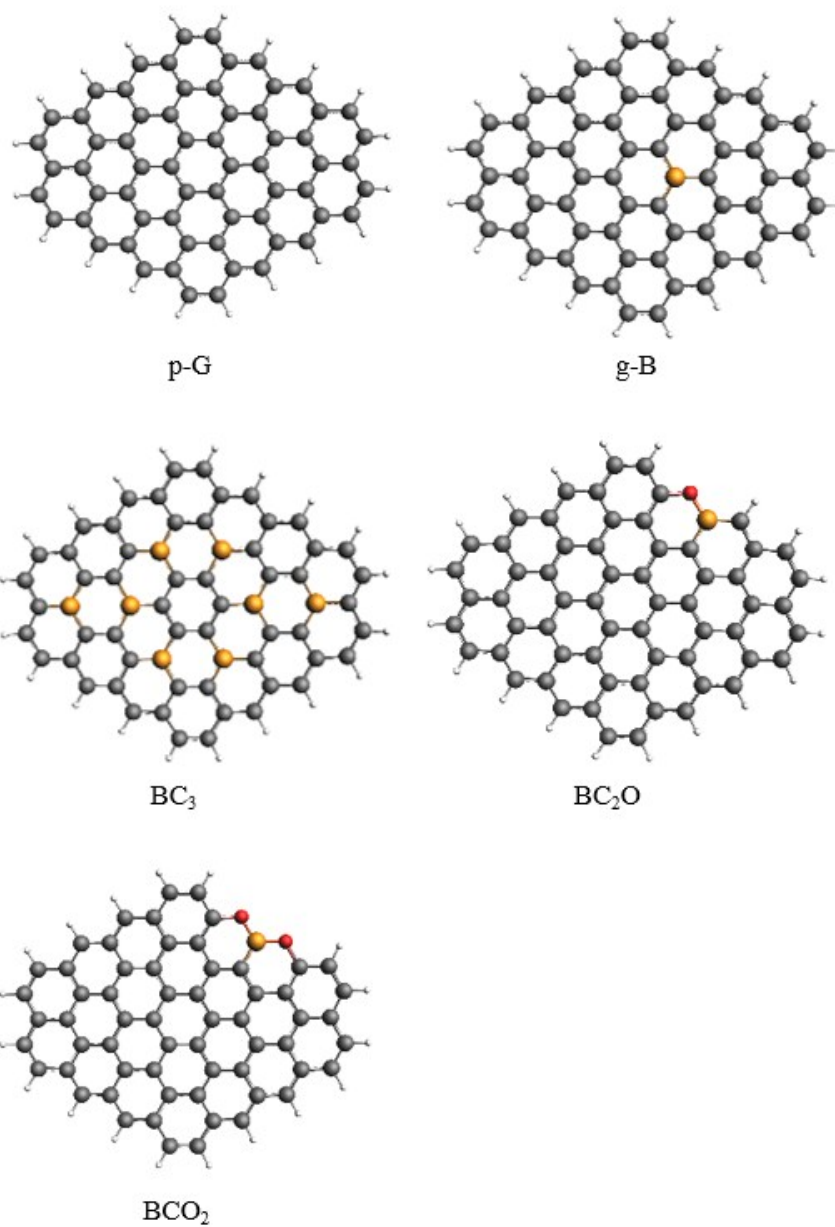


Figure S7 Optimized structures of p-G and B-doping models.

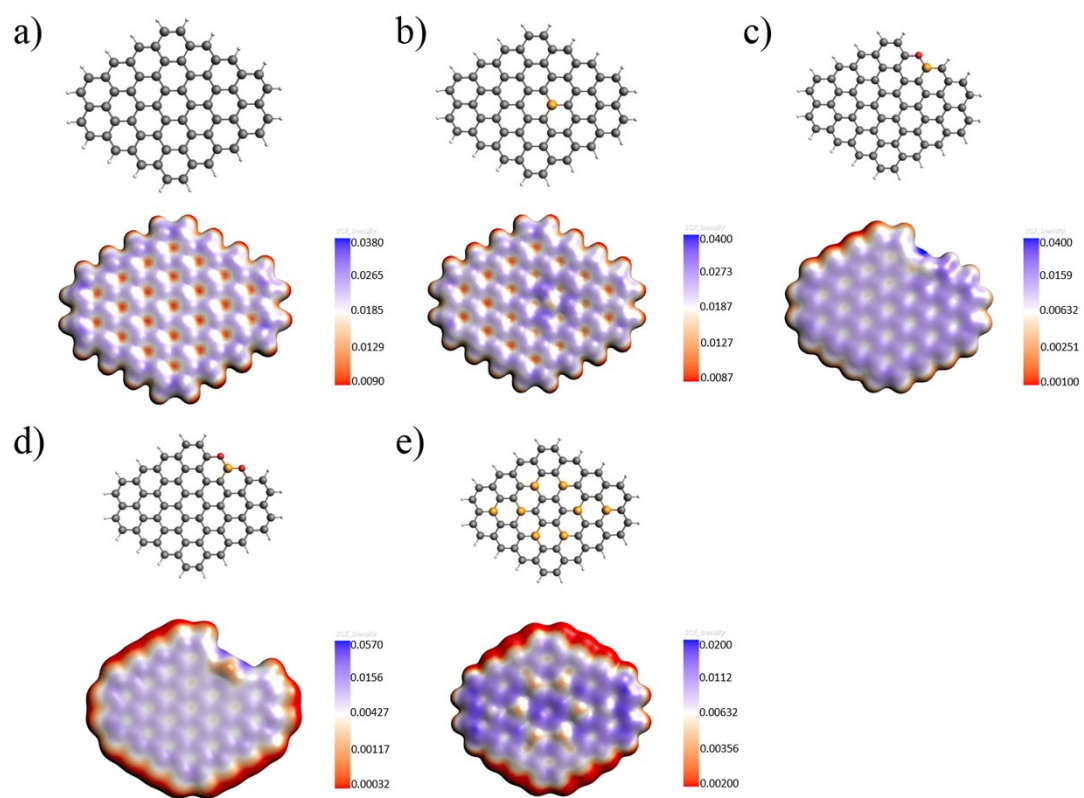


Figure S8 Electrostatic potential mapping over various surface a) p-G, b) g-B, c) BC_2O , d) BCO_2 , and e) BC_3 . Red color represents negative potential and blue color represents positive potential.

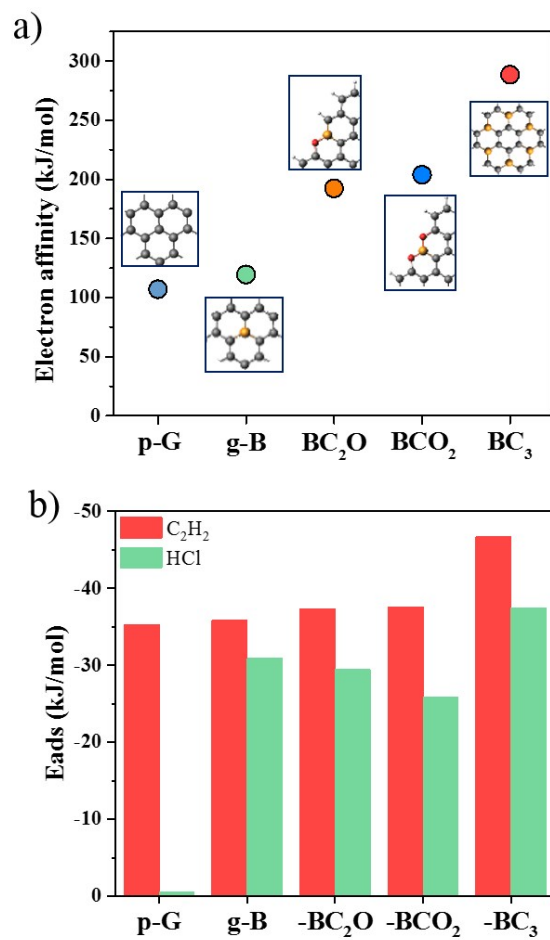


Figure S9 a) The electron affinity and b) the adsorption energies (E_{ads}) of C_2H_2 and HCl over p-G surface and four kinds of B-doped surface.

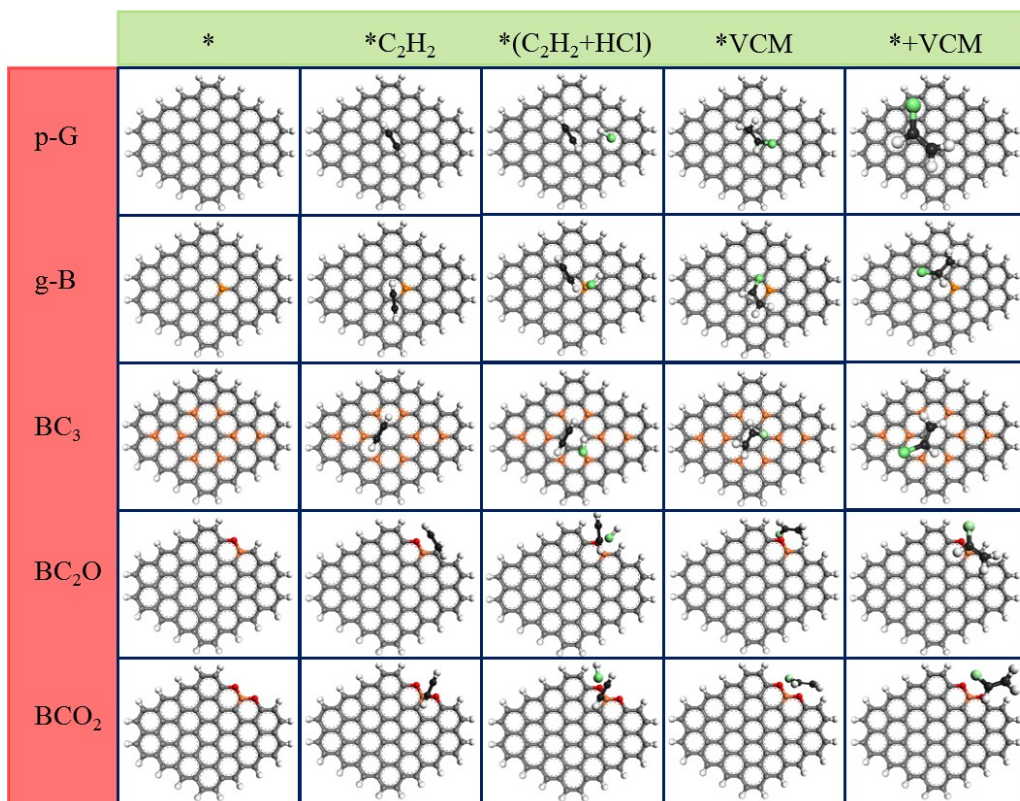


Figure S10 The reaction pathway on the five different active sites.

References

1. F. Sun, Z. Qu, J. Gao, H. B. Wu, F. Liu, R. Han, L. Wang, T. Pei, G. Zhao and Y. Lu, *Adv. Fun. Mat.*, 2018, **28**, 1804190.
2. N. Sreekanth, M. A. Nazrulla, T. V. Vineesh, K. Sailaja and K. L. Phani, *Chem. Commun.*, 2015, **51**, 16061.
3. Z. Zhou, X. Niu, L. Ma and J. Wang, *Adv. Theory Simul.*, 2019, **2**, 1900074.
4. J. Feng, H. Dong, L. Yu and L. F. Dong, *J. Mater. Chem. C*, 2017, **5**, 5984.
5. X. Niu, Y. Li, H. Shu and J. Wang, *Nanoscale*, 2016, **8**, 19376.
6. X. Niu, H. Shu, Y. Li and J. Wang, *J. Phys. Chem. Lett.*, 2017, **8**, 161.
7. H. Tanaka, Y. Kawamata, H. Simizu, T. Fujita, H. Yanagisawa, S. Otani and C. Oshima, *Solid State Commun.*, 2005, **136**, 22.
8. X. Li, Y. Wang, L. Kang, M. Zhu and B. Dai, *J. Catal.*, 2014, **311**, 288.
9. X. Li, X. Pan and X. Bao, *J. Energy Chem.*, 2014, **23**, 131.
10. X. Wang, B. Dai, Y. Wang and F. Yu, *ChemCatChem*, 2014, **6**, 2339.
11. X. Li, X. Pan, L. Yu, P. Ren, X. Wu, L. Sun, F. Jiao and X. Bao, *Nat. Commun.*, 2014, **5**, 3688.
12. B. Dai, K. Chen, Y. Wang, L. Kang and M. Zhu, *ACS Catal.*, 2015, **5**, 2541.
13. C. Zhang, L. Kang, M. Zhu and B. Dai, *RSC Adv.*, 2015, **5**, 7461.
14. Y. Yang, G. Lan, X. Wang and Y. Li, *Chin. J. Catal.*, 2016, **37**, 1242.
15. X. Li, J. Zhang and W. Li, *J. Ind. Eng. Chem.*, 2016, **44**, 146.
16. T. Zhang, J. Zhao, J. Xu, J. Xu, X. Di and X. Li, *Chin. J. Chem. Eng.*, 2016, **24**, 484.
17. P. Li, H. Li, X. Pan, K. Tie, T. Cui, M. Ding and X. Bao, *ACS Catal.*, 2017, **7**, 8572.
18. S. Chao, F. Zou, F. Wan, X. Dong, Y. Wang, Y. Wang, Q. Guan, G. Wang and W. Li, *Sci. Rep.*, 2017, **7**, 39789.
19. K. Zhou, B. Li, Q. Zhang, J. Q. Huang, G. L. Tian, J. C. Jia, M. Q. Zhao, G. H. Luo, D. S. Su and F. Wei, *ChemSusChem*, 2014, **7**, 723.
20. G. Lan, Y. Wang, Y. Qiu, X. Wang, J. Liang, W. Han, H. Tang, H. Liu, J. Liu, Y. Li, *Chem. Commun.*, 2018, **54**, 623.
21. J. Wang, F. Zhao, C. Zhang, L. Kang and M. Zhu, *Appl. Catal. A Gen.*, 2018, **549**, 68.
22. G. Lan, Y. Qiu, J. Fan, X. Wang, H. Tang, W. Han, H. Liu, H. Liu, S. Song, Y. Li, *Chem. Commun.*, 2019, **55**, 1430.
23. R. Lin, S. K. Kaiser, R. Hauert and J. Pérez-Ramírez, *ACS Catal.*, 2018, **8**, 1114.
24. J. Wang, W. Gong, M. Zhu and B. Dai, *Appl. Catal. A Gen.*, 2018, **564**, 72.
25. W. Liu, M. Zhu and B. Dai, *New J. Chem.*, 2018, **42**, 20131.
26. X. Qiao, Z. Zhou, X. Liu, C. Zhao, Q. Guan and W. Li, *Catal. Sci. Technol.*, 2019, **9**, 3753.
27. Y. Qiu, S. Ali, G. Lan, H. Tong, J. Fan, H. Liu, B. Li, W. Han, H. Tang, H. Liu and Y. Li, *Carbon*, 2019, **146**, 406.
28. S. Mei, J. Gu, T. Ma, X. Li, Y. Hu, W. Li, J. Zhang and Y. Han, *Chem. Eng. J.*, 2019, **371**, 118.
29. J. Zhao, B. Wang, Y. Yue, G. Sheng, H. Lai, S. Wang, L. Yu, Q. Zhang, F. Feng, Z.-T. Hu and X. Li, *J. Catal.*, 2019, **373**, 240.
30. X. Dong, S. Chao, F. Wan, Q. Guan, G. Wang and W. Li, *J. Catal.*, 2018, **359**, 161.